International Conference on Applied Energy 2020
Dec. 1 - Dec. 10, 2020, Bangkok / Virtual
Paper ID: 191

Application of a new type of Lithium-Sulfur battery in plug-in hybrid electric vehicle cruise control

Yiming Ye[1], Jiangfeng Zhang[1*], Srikanth Pilla[1], and Apparao M Rao[2]

1 Department of Automotive Engineering, Clemson University, Greenville, SC 29607, USA

2 Clemson Nanomaterials Institute, Department of Physics and Astronomy, Clemson University, Clemson, South Carolina 29634, USA

ABSTRACT

This paper analyzes the application of a novel Lithium-Sulfur (Li-S) battery with the bilateral solid electrolyte interface to the cruise control of plug-in hybrid electric vehicles (PHEVs). An optimal cruise control strategy based on the dynamic programming algorithm is modified to include battery degradation cost during energy management. The degradation cost of a Lithium-ion Battery is used as a benchmark to analyze the degradation cost of Li-S battery of PHEVs. The comparison results demonstrated that the application of the new Li-S battery significantly reduces the cost of PHEVs.

Keywords: Li-S battery, Plug-in hybrid vehicle, Battery degradation, Energy management strategy

1. INTRODUCTION

Lithium-ion batteries (LiBs) have been the only choice of batteries for hybrid electric vehicles (HEVs) and plug-in electric vehicles (PHEVs). Although these electric vehicle technologies are developing quickly, the automobile market is still dominated by internal combustion engine (ICE) vehicles. There are many reasons for this phenomenon, such as distrust in new technology, robustness, and reliability of ICE vehicles. One of the main reasons, however, is that the cost of PHEVs is much higher than ICE equivalents due to the expensive cost of LiBs. The LiBs not only have an expensive initial capital cost but also degrade significantly that makes the entire PHEVs depreciate faster than a conventional ICE vehicle.

To solve the high-cost problem of LiBs, technologies for other types of batteries gain significant attention of researchers and industry. Li-S batteries, as one of the alternatives, have the advantage of low-cost sulfur materials and very high energy density - almost six times of the current LiBs technology [1]. However, these Li-S batteries also have drawbacks that limit their ability to be commercialized for PHEVs. The main disadvantages are the low power output and short battery lifetime [2]. The low power output can be accommodated by adequately selecting an ultracapacitor to boost electrical power output to the traction motor of the vehicle for additional acceleration [3]. The short battery life is due to dendrite growth on the anode and shuttle effect of the cathode caused by inferior electrodes, separators, and electrolytes [4]. Recently, a new Li-S battery with bilateral solid electrolyte interphase (SEI) layers is reported in which mixed electrolytes promoted the simultaneous growth of SEI on both electrodes thus preventing the dendrite growth on the lithium anode and the shuttle effect on the sulfur cathode [4].

This study will explore the energy consumption cost-saving benefits of replacing LiBs by the aforementioned bilateral SEI Li-S battery technology for PHEV cruise control. The LiB technology will be used as a benchmark to evaluate the Li-S battery performance. The higher energy density will provide more driving range with less degradation cost, which effectively reduces the initial capital cost and increases the lifespan of PHEVs.

2. MODELING METHODOLOGY

2.1 Modeling of PHEVs

The hybrid power is mainly provided by ICE and electric motor, and the produced power flows through the powertrain system to the wheels. The power output of the ICE and electric motor can be flexibly adjusted according to the state of charge (SOC) of the battery, the

*: Corresponding Author, email: jiangfz@clemson.edu

driver's power demand, and the current driving conditions of the vehicle so that PHEVs have different driving modes. The structure and the basic parameters of the PHEV model are shown in Fig. 1 and Table 1.

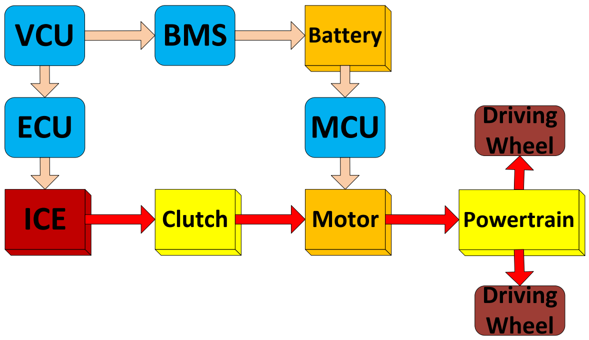

Fig. 1. The structure of the PHEV model.

Table 1. Parameters of the PHEV model.

Parameters	Value
Curb weight (kg)	1800
Max weight (kg)	2180
Windward area (m^2)	2.34
Air resistance coefficient	0.30
Wheelbase (m)	2870
Location of centroid	3/7
Wheel radius(mm)	668.3
Top speed (km/h)	150
0-100 km/h time (s)	10
Grade ability (%)	30

The hybrid power system converts the stored energy into the kinetic energy and potential energy of the vehicle in the process of propelling the vehicle. Besides, air resistance and rolling resistance are also continually consuming energy [5]. The energy balance is shown in Eq. (1).

$$P_{trac}(t) = P_{\text{inertia}}(t) + P_{roll}(t) + P_{aero}(t) + P_{grade}(t) \quad (1)$$

$$P_{inertia}(t) = M_{veh} v'_{veh}(t) v_{veh}(t) \quad (2)$$

$$P_{roll}(t) = M_{veh} g f_{roll}(v_{veh}, p_{tire}, \cdots) v_{veh}(t) \cos\delta(t) \quad (3)$$

$$P_{aero}(t) = \frac{1}{2}\rho_a A_f C_d (v_{veh}(t))^3 \quad (4)$$

$$P_{grade}(t) = M_{veh} g v_{veh}(t) \sin\delta(t) \quad (5)$$

where $P_{trac}(t)$ is the power provided by traction, $P_{\text{inertia}}(t)$ is the power to propel the PHEV, $P_{roll}(t)$ is the power consumed by rolling resistant, $P_{aero}(t)$ is the power consumed by air resistant, $P_{grade}(t)$ is the power consumed by road grade, M_{veh} is the total mass of the PHEV, $v_{veh}(t)$ is the driving speed, g is the acceleration of gravity, $f_{roll}(v_{veh}, p_{tire}, \cdots)$ is the coefficient of rolling resistance, $\delta(t)$ is the road grade, ρ_a is the density of air, A_f is windward area, and C_d is coefficient of air resistance.

2.2 The Battery model

Using the data presented in the study above about experimental electrolyte compounds for Li-S batteries, a battery degradation model is obtained with a simple linear fitting function [4]. The data are first approximated and plotted for the overall capacity and coulombic efficiency of the best performing electrolyte compound as they are related to the number of charging cycles. The information for the capacity and coulombic efficiency to 2500 cycles is shown in Fig. 2. It also offers a fitting function, which is provided in Eq. (6).

$$Capacity = 677.28 - 0.0203x \quad (6)$$

where capacity is the remaining capacity in mAh/g, and x is the cycle number.

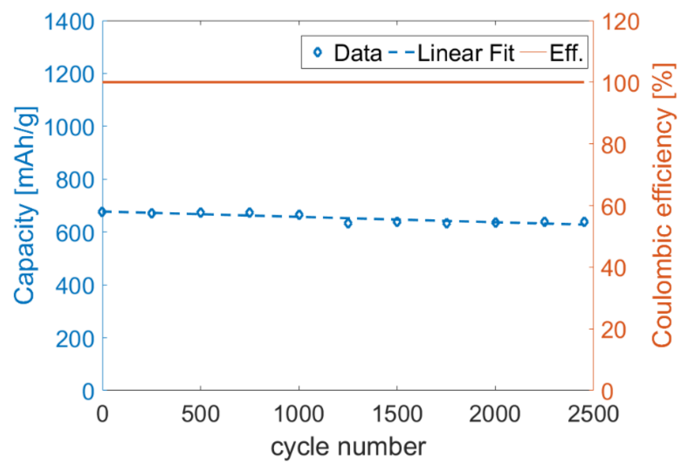

Fig. 2. Battery degradation.

The degradation cost model is considered as a semi-empirical model, which is proposed in Ref. [6]. The model is shown in Eq. (7).

$$Q_{bat} = C_{bat} E_{nom} Ah_{cycle} / Ah_{allow} \quad (7)$$

where C_{bat} is the battery pack cost per unit energy, E_{nom} is the battery nominal energy capacity, Ah_{allow} is the allowable battery Ampere-hour number and is shown in Eq. (8), and Ah_{cycle} is the battery throughput number of Ampere-hour in each operation cycle [7].

$$Ah_{allow} = \left(\frac{0.2}{A} * \exp\left(-\frac{E_a + B * C_{Rate}}{R * T_{Bat}}\right)\right)^{\frac{1}{Z}} \quad (8)$$

where C_{Rate} is the average discharge rate in the circle T_{Bat} is the battery temperature B is the compensate factor R is the gas constant Z is power law factor. The parameters in Eq. (8) are presented in Table 2.

Table 2. Battery degradation parameters.

A	E_a	B	R	Z
0.0032	15162	1516	8.3144598	0.824

2.3 Driving cycle

Driving cycles are a prerequisite for matching PHEVs' power system parameters and formulating energy management strategies that have guiding significance for the development of PHEVs. This study consider the Urban Dynamometer Driving Schedule (UDDS) as the input signal to drive the PHEV model [8]. The single UDDS driving cycle is not enough to deplete the battery, so there is a concatenation of the UDDS driving cycle with 64.3 km total driving range, which is shown in Fig. 3. During the sequential UDDS driving cycle, the state of charge (SOC) decreases from 100% to nearly 10%.

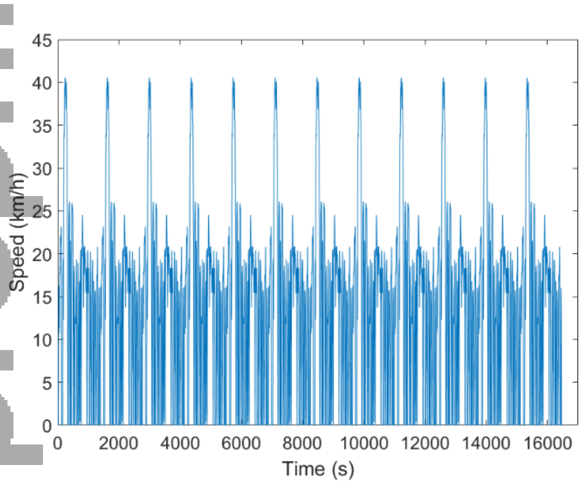

Fig. 3. Input signal of PHEV model.

2.4 Energy management

The PHEV model constructed in this study can be described by a discrete-time nonlinear system. The discretization of the driving cycle is used as the prior information of the system. The battery SOC is regarded as the system state variable, and the ICE output torque is taken as the system control variable. The system state transition equation is shown in Eq. (9).

$$soc(k+1) = T_k(soc(k), T_e(k)) \quad (9)$$

where $soc(k+1)$ is the system state variable at k+1 state, and $T_k(soc(k), T_e(k))$ is the state transition function at *k*-th state.

The cost function of the energy management strategy is shown in Eq. (10).

$$J(x_0, u) = \min(L_N(x_N) + \sum_{k=1}^{N-1} L_k(x(k), u(k))) \quad (10)$$

where $L_N(x_N)$ is the fuel consumption at the final time instant *N* and $L_k(x(k), u(k))$ is the instantaneous fuel consumption at instant *k*.

For a stable operation of the system, the state variable and control variable must satisfy the following boundary constraints:

$$\begin{cases} n_{ICE\_\min} \le n_{ICE}(k) \le n_{ICE\_\max} \\ T_{ICE\_\min} \le T_{ICE}(k) \le T_{ICE\_\max} \\ n_{EM\_\min} \le n_{EM}(k) \le n_{EM\_\max} \\ T_{EM\_\min} \le T_{EM}(k) \le T_{EM\_\max} \end{cases} \quad (11)$$

3. RESULTS AND ANALYSIS

The PHEV model constructed in the previous section is operated continuously for 1000 cycles. Figs. 4 and 5 show the SOC changes during the first cycle and the last cycle of the PHEV model with LiBs and Li-S battery as the electric power source.

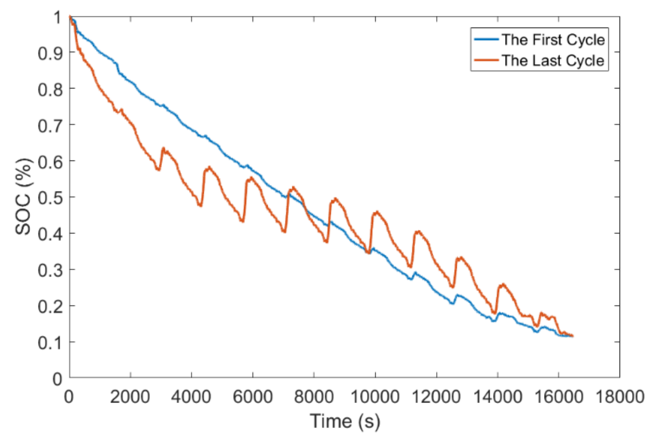

Fig. 4. The SOC with LiBs.

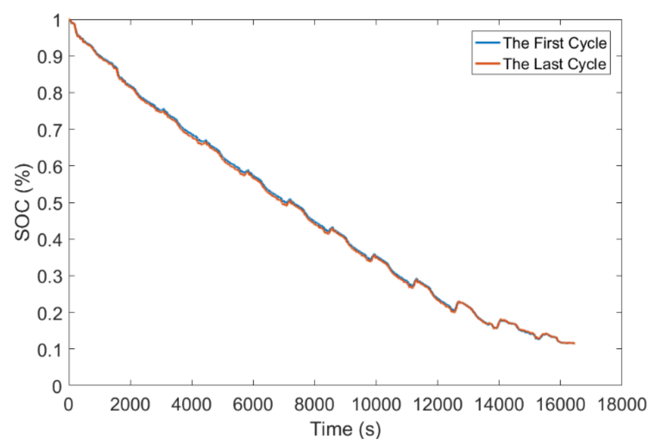

Fig. 5. The SOC with Li-S battery.

It can be seen from Fig. 4 that due to the severe degradation of LiBs, the PHEV model that uses LiBs as the electric power source consumes electricity too fast in the last cycle, which causes ICE to intervene to provide the power for PHEV and to charge the battery frequently. Fig. 5 indicates that the Li-S battery has only minimal degradation in 1000 cycles, so the SOC change curves of the first cycle and the last cycle of the PHEV model using Li-s battery are consistent.

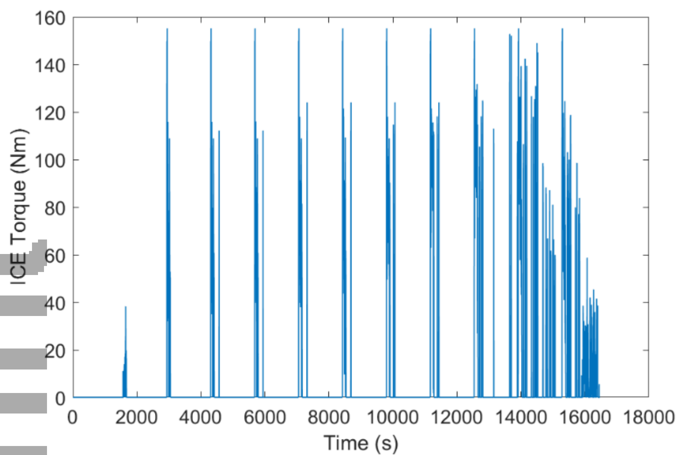

Fig. 6. The ICE torque with Li-S battery in the last cycle.

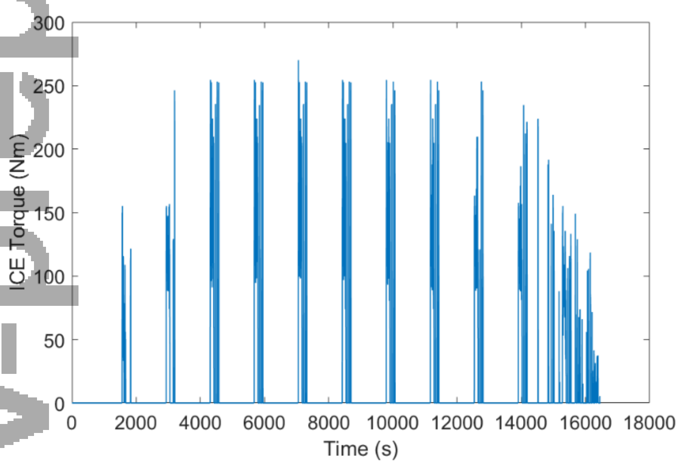

Fig. 7. The ICE torque with LiBs in the last cycle

The Fig. 6 shows the torque provided by the ICE of PHEV with Li-S battery in the last cycle. The proportion of ICE provided power accounts for 10.45% in the entire cycle and the average torque is 66.65 Nm. Fig. 7 illustrates the ICE torque of PHEV with LiBs in the last cycle. The proportion of ICE provided power accounts for 12.48% in the last cycle and the average torque is 116.07 Nm. A comparison between the data in Figs. 6 and 7 suggests that the ICE in the PHEV with a Li-S battery is required to provide smaller torque and also run less frequently than the case with a LiB. This implies that more power will be drawn from the battery in case Li-S is employed, which is a plus for the fuel economy. Furthermore, the Li-S battery degradation cost is 94.1% less than LiB.

4. CONCLUSION

This study explored the use of a new Li-S battery with bilateral SEIs in PHEV cruise control. With regards to the cost of battery degradation, the degradation of a LiB is used as a benchmark to evaluate the performance of the Li-S battery in PHEVs. Concatenated UDDS driving cycles are adopted in the energy calculation. The PHEV model is operated with a cruise control based on the DP algorithm for 1000 times for battery degradation effects to occur. The comparison case study demonstrates that the new Li-S battery can save 94.1% degradation costs for PHEVs compared to a LiB.

ACKNOWLEDGMENT

This study is sponsored by the NASA EPSCoR Program under Award #NNH17ZHA002C.

REFERENCE

[1] Mourembles D, Buergler B, Gajewski L, et al. Li-S Cells for Space Applications (LISSA).2019 European Space Power Conference (ESPC). IEEE, 1-5.

[2] Fotouhi A, Auger D J, Propp K, et al. Lithium-Sulfur Battery State-of-Charge Observability Analysis and Estimation. IEEE Transactions on Power Electronics, 2017, 33(7): 5847-5859.

[3] Sun L. a novel battery-supercapacitor power supply for electric vehicles (EVs) – design, simulation and experiment. http://hdl.handle.net/10453/120203

[4] Fan L, Chen S, Zhu J, et al. Simultaneous suppression of the dendrite formation and shuttle effect in a lithium-sulfur battery by bilateral solid electrolyte interface. Advanced Science, 2018, 5(9): 1700934.

[5] Onori S, Serrao L, Rizzoni G. Hybrid electric vehicles: Energy management strategies. London: Springer, 2016.

[6] Song Z, Li J, Han X, et al. Multi-objective optimization of a semi-active battery/supercapacitor energy storage system for electric vehicles. Applied Energy, 2014, 135: 212-224.

[7] Feng Y, Dong Z. Optimal energy management strategy of fuel‐cell battery hybrid electric mining truck to achieve minimum lifecycle operation costs. International Journal of Energy Research.

[8] Martel F, Kelouwani S, Dubé Y, et al. Optimal economy-based battery degradation management dynamics for fuel-cell plug-in hybrid electric vehicles. Journal of Power Sources, 2015, 274: 367-381.